

Effect of High Density Electric Current Pulse on Solidification of Cu-37.4 wt.%Pb Monotectic Alloy Melt

Teng MA¹, Guihong GENG², Xiaosi SUN³, Xi HAO⁴, Weixin HAO^{5*}

¹ School of Mathematics, Jinzhong University, Jinzhong 030619, Shanxi, China

² School of Materials Science and Engineering, North Minzu University, Yinchuan 750000, Ningxia, China

³ Department of Metallurgy and Environmental Engineering, Shanxi Engineering Vocational College, Taiyuan 030002, Shanxi, China

⁴ The Coordinative Innovation Centre of Taiyuan Heavy Machinery Equipment, Taiyuan University of Science and Technology, Taiyuan 030024, Shanxi, China

⁵ School of Materials Science and Engineering, Taiyuan University of Science and Technology, Taiyuan 030024, Shanxi, China

crossref <http://dx.doi.org/10.5755/j01.ms.26.1.21060>

Received 27 June 2018; accepted 29 September 2018

The effect of high-density electric current pulse (ECP) on the solidification of Cu-37.4 wt.%Pb monotectic alloy melt was investigated. The microstructure formation mechanisms of ECP were clarified according to liquid metal cluster theory. The results demonstrated that with ECP treatment, the microstructure of Cu-Pb monotectic alloy became finer, the distribution of Pb phase in the matrix was more even and the solute trapping was significantly apparent. Based on the metal liquid cluster theory under ECP, the solid solubility increase result might be due to the salvation clusters increase under the action of pulse current, leading to the binding force increase among solute atoms and solvent atoms. Simultaneously, the aforementioned results were verified through the Differential Scanning Calorimetry (DSC) curve analysis. The results of hardness test, anti-friction test and wear-resistance test show that the ECP can enhance the hardness, improve the properties of anti-friction and wear-resistance of the alloy.

Keywords: electric current pulse, solidification, grain refinement, solid solubility, Cu-Pb monotectic alloy.

1. INTRODUCTION

Due to the excellent wear resistance and superconducting properties, Cu-Pb alloys are considered as advanced bearings materials if the soft Pb phase is dispersed in a hard matrix of Cu [1]. Adversely, the Cu-Pb phase diagram is characterized by the appearance of a miscibility gap in the liquid state [2, 3]. When a homogeneous liquid is cooled into the miscibility gap, the components are no longer miscible and consequently two liquid phases develop. It is difficult to obtain a uniform and fine alloy structure, severely affecting the material properties of the alloy. A significant amount of research was carried out to investigate this drawback, while the segregation in the solidification structure was avoided through certain techniques, but the progress is still slow due to the higher cost and technological difficulties [4, 5].

High-density electric current pulses (ECP) demonstrate high effects on the solidification behaviour. [6, 7]. The ECP can improve the heterogeneous nucleation rate of a liquid or semi-liquid metal, promoting the solute redistribution and refining the solidification microstructure [8–10]. The effects of ECP treatment on the solidification structure of pure metals [6, 11] and eutectic alloys [5, 12] were studied in most recent researches. Adversely, the effect of ECP treatment on monotectic alloys has rarely been reported. Simultaneously, many researchers have investigated the solidification microstructure refinement

through ECP, but few reports exist on the effect of ECP treatment on the solid solubility of alloys. It is generally considered that the liquid structure transition plays an important role to the alloy ingot grain refinement, and many experiments have indicated that the metal casting structure is most closely related to its liquid matrix [13].

In this paper, the solidification microstructure evolution of Cu-37.4 wt.%Pb monotectic alloy treated with ECP was investigated. Furthermore, based on liquid metal cluster theory [14], the grain refinement resulting from ECP was studied. Based on the excellent wear resistance of Cu-Pb alloy, the hardness test, anti-friction test and wear-resistance test of Cu-Pb alloy under ECP treatment were carried out. It was proved that the electric pulse can enhance the hardness of Cu-37.4wt.%Pb alloy and improve the properties of anti-friction and wear-resistance of the alloy.

2. EXPERIMENTAL APPARATUS AND PROCEDURE

The experimental apparatus consisted of the customized pulse power supply, the vacuum system, the high frequency induction heating device and the temperature measurement system (Fig. 1). In order to reduce heterogeneous nucleation, a customized boron nitride conductive electrode (chemical composition: BN+TiB₂+AlN) of 100 W/mk in thermal conductivity was designed and connected to the molybdenum (Mo) electrode (Fig. 2). Cu and Pb particles were mixed in a ratio of

* Corresponding author. Tel.: +8613503505572.
E-mail address: wxhao@vip.sina.com (W.X. Hao)

68.6:37.4 (Cu:Pb in wt.%). These were consequently placed into the cylindrical boron nitride crucible (Fig. 2).

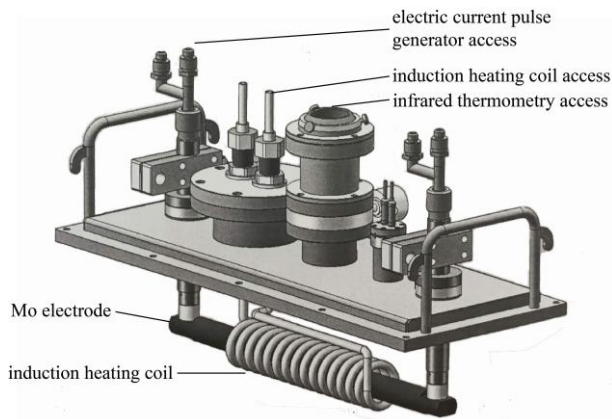


Fig. 1. Schematic drawing of the experimental setup

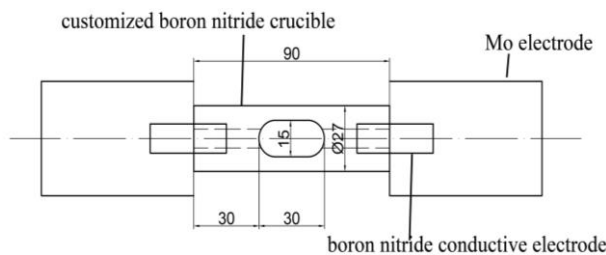
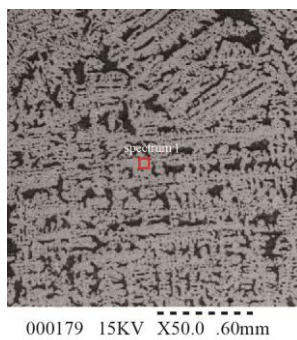
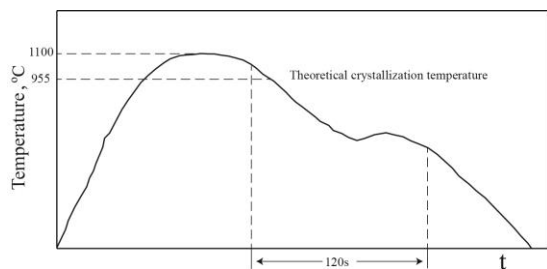


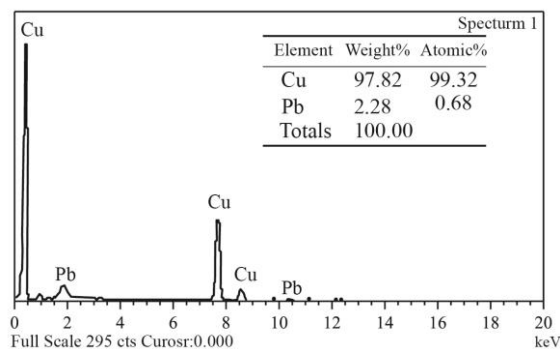
Fig. 2. Schematic sketch of the crucible and the electrodes

Table 1. Parameters of pulsed current

Sample	Current peak, A	Voltage, V	Current frequency, Hz	Pulse width, μ s
a	800	27	30	20
b	1000	33	30	20
c	1200	40	30	20
d	1400	47	30	20



a



b

Fig. 4. Solidification and the energy spectrum analysis of Cu-37.4 wt.% Pb monotectic alloys without applied ECP: a – solidification structure; b – energy spectrum analysis

Fig. 3. Schematic diagram of the action time of the ECP on the molten metal

The samples were cyclically overheated to 1200 K for 5 min under Ar atmosphere with a high-frequency induction heating device. The ECP treatment was performed when the boron nitride conductive electrode end was horizontally in contact with the molten metal. The parameters of pulsed currents are listed in Table 1. Numerous studies [15–16] had shown that the optimization effect of solidification structure was more significant with the increase of current density, especially in the high-density current conditions, the solidification structure will be greatly improved. For the pulse width, since the high-frequency oscillation attenuation and relaxation time of the low pulse width pulse current were very short, the influence of the Joule heating effect brought about by them can be ignored. Therefore, the current parameters of small pulse width with high frequency were used in this experiment. Where, the current density can be up to $6 \times 10^6 \text{ A/m}^2 \div 2 \times 10^7 \text{ A/m}^2$ by changing the peak current. Fig. 3 presents the action time schematic diagram of the pulse current on the molten metal.

The effects of ECP on the solidification behavior and phase transition of Cu-37.4 wt.%Pb monotectic alloy were analyzed with a TGA/DSC1 synchronous thermal analyzer (Quintest, FL, USA). Continuous heating and cooling DSC experiments were carried out with an aluminum pan at the rate of 10 K/min at the temperature range of room temperature to 1600 °C.

The 10 mm piece test sample was cut from the solidified specimen and consequently polished for metallographic examination. The etching reagent used to reveal the macrostructure was composed of 80 % of anhydrous alcohol, 10 % of hydrochloric acid and 10 % w/v of ferric chloride. The microstructures of Cu-37.4wt.%Pb monotectic alloys were observed through scanning electron microscopy (SEM) (JSM6510, JEOL, Tokyo, Japan) along the center line of the specimens. Energy dispersive spectroscopy (EDS) tests were performed with an OXFORD X-Max N spectrometer.

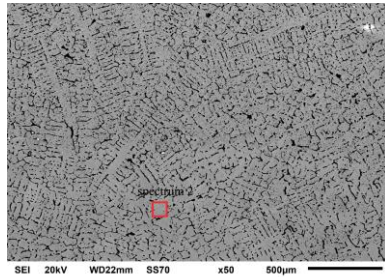
The samples prepared at different pulse current peaks were polished and inserted. Hardness was tested by HV-120 Vickers hardness tester, with loading load of 5 kgf and loading time of 15 s.

Under the same conditions, 5 points of the same sample were selected for testing, and the average value was taken as the hardness value of the sample. The friction coefficient and wear rate of Cu-37.4 wt.%Pb was tested on SRV friction and wear tester.

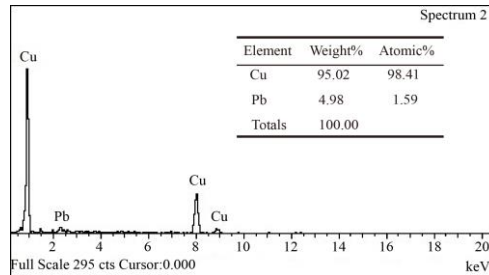
3. RESULTS AND DISCUSSION

The reference experiment conducted without applied ECP (Fig. 4 a) shows that in solidification of Cu-37.4 wt.%Pb alloy, there were coarse dendrites of the

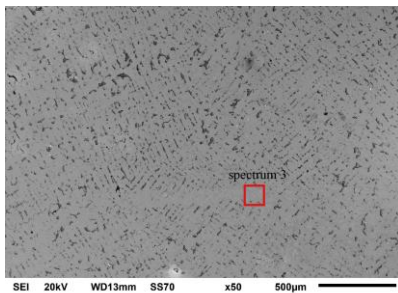
α (Cu) phase and unidirectional solidified structure found, as well as the large Pb phase distributed between α (Cu) dendrites. The microstructures of Cu-37.4 wt.%Pb alloys in the longitudinal section, treated with differential ECPs are presented in Fig. 5. When the ECP treatment with $I = 800$ A was applied, the solidification structure of Cu-37.4wt.%Pb monotectic alloys possessed a good overall homogeneity of the microstructures, in which, the α (Cu) dendrites grown at different orientations and their primary arms were relatively tiny.



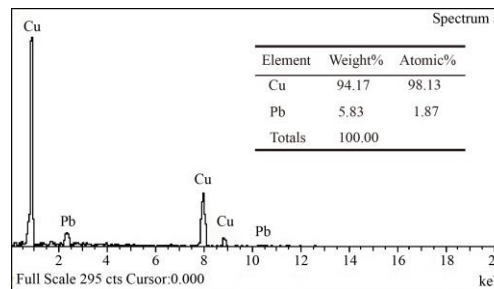
a



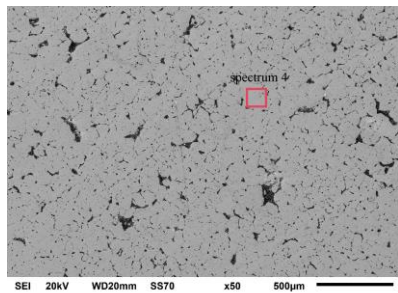
b



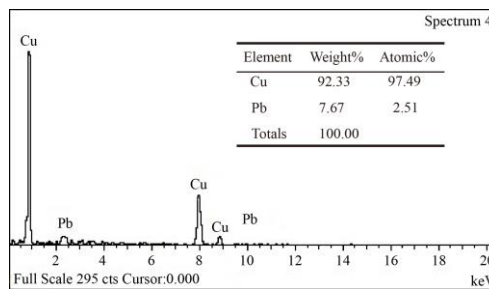
c



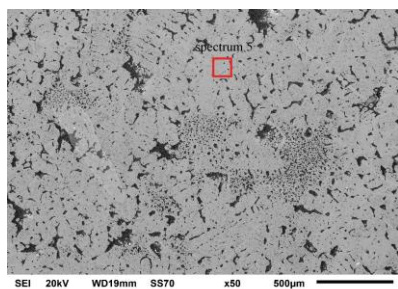
d



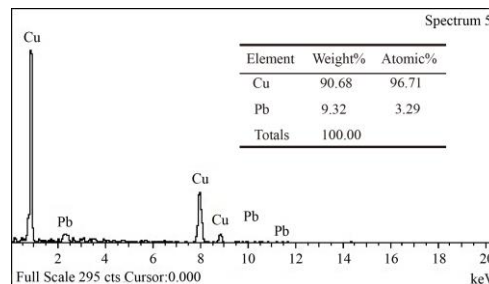
e



f



g



h

Fig. 5. Solidification structure and energy spectrum analysis of alloy structures, treated with different pulse current: a, b – $I = 800$ A; c, d – $I = 1000$ A; e, f – $I = 1200$ A; g, h – $I = 1400$ A

Also, the Pb was dispersed uniformly within the $\alpha(\text{Cu})$ dendrites without visible macro segregation (Fig. 5 a). When the current intensity increased to $I = 1000$ A, the solidification structures of Cu-37.4 wt.%Pb monotectic alloys were further refined, characterized by shorter primary arms and lower spacing of $\alpha(\text{Cu})$ dendrites (Fig. 5 c). When $I = 1200$ A, the solidification structures improved with a certain amount of $\alpha(\text{Cu})$ having transitioned from dendrites to flocculus, along with the dissociation and coagulation of the Pb phase in $\alpha(\text{Cu})$ dendrites (Fig. 5 e). This demonstrated that an increased amount of the Pb phase existed in the Cu matrix. Moreover, low-sized Pb particles were dispersed in the Cu matrix, due to solute trapping effects during the rapid solidification.

When the peak current increased up to 1400 A, the flocculent Pb appeared in the Cu matrix (shown in Fig. 5 f), indicating that the solute trapping was more apparent.

Energy spectrum analysis was performed subsequently to the alloy treatment with different pulse currents or without ECP treatment, in order to further investigate the ECP effect on the solidification structures of the Cu-37.4 wt.%Pb monotectic alloy. As presented in Fig. 4 b, the $\alpha(\text{Cu})$ matrix in the solidified structure contained 97.82 % of Cu and 2.18 % of Pb without the ECP treatment. Fig. 4 d, f, h and j presents that the degree of solid solution of solute Pb in the Cu matrix increased as the peak current increased. Based on the aforementioned results, it was inferred that the ECP could significantly enhance the solute trapping effect in the solidification structure of the Cu-37.4wt.%Pb monotectic alloy. As the ECP peak value of the gradually increased, the solute trapping effect became more discrete.

The differential scanning calorimetry (DSC) test results of the samples with ECP or without ECP are presented in Fig. 6, which reflected the heating and cooling behavior of the Cu-37.4 wt.%Pb monotectic alloy, providing more information on the melt structure changes under various conditions. Table 2 presents the thermodynamic function values calculated based on the DSC curve of each sample. In Fig. 6 a, it was noted that the melting temperature of the unmodified sample was 956.3 °C and according to the specular equation, the latent heat of fusion was 202.1 J/g through calculation. Subsequently to different peak currents ($I = 800$ A, $I = 1000$ A, $I = 1200$ A, $I = 1400$ A), the melting temperatures of the metals were 956.1 °C,

956.3 °C, 955.8 °C and 955.7 °C, respectively, with the corresponding calculated latent heat of fusion values of 170.8 J/g, 163.9 J/g, 149.3 J/g and 138.5 J/g. Apparently, compared to the unmodified samples, the melting temperatures of modified samples with different peak currents slightly changed, whereas the latent heat of fusion was significantly reduced. As presented in the cooling curve (Fig. 6 b), the solidification temperature of the sample without ECP treatment was 956.3 °C, while the released latent heat of crystal was 210.8 J/g. The solidification temperatures of the samples with ECP treatment decreased, while the release of latent heat of the crystal was significantly reduced. When the peak currents were $I = 800$ A, $I = 1000$ A, $I = 1200$ A, $I = 1400$ A, the released latent heat values of crystallization were 180.4 J/g, 172.6 J/g, 155.3 J/g and 147.2 J/g. As the ECP peak value increased, the release of latent heat of crystallization was reduced. As it could be observed from Fig. 6 b, the undercooling of the melt significantly increased through ECP treatment. Also, as the peak current increased, the undercooling continuously increased. When the peak current value was 1400 A, the Cu-Pb alloy melt undercooling degree was 180 K, which was increased by an order of magnitude compared to the previous studies [12, 14].

The Cu-37.4 wt.%Pb monotectic alloy was immiscible. Therefore, the microstructure depended on the liquid-liquid phase transformation in the miscibility gap [1]. The result indicated that ECP treatment might affect the microstructure formations of the alloy and the spatial motions of the precipitated phase droplets of Pb. According to liquid metal cluster theory [12, 17], the microstructure formation and the affecting mechanisms of ECP were clarified as follows.

The atoms and metal clusters existed in the metal melt. According to liquid metal cluster theory, when ECP was applied to the metal melt, the potentials of one side of the metal cluster external layer were reduced, due to repeated distortion and relaxation of the external layer of the cluster (the outer layer of the metal cluster would be repeatedly deformed and relaxed, resulting in a decrease in the electric potential of one side of the outer layer). This would lead to the interaction enhancement among the cluster and the surrounding liquid metal atoms, reducing the “barriers” of the combination of atoms and metal clusters, as well as promoting the combination of clusters and surrounding atoms.

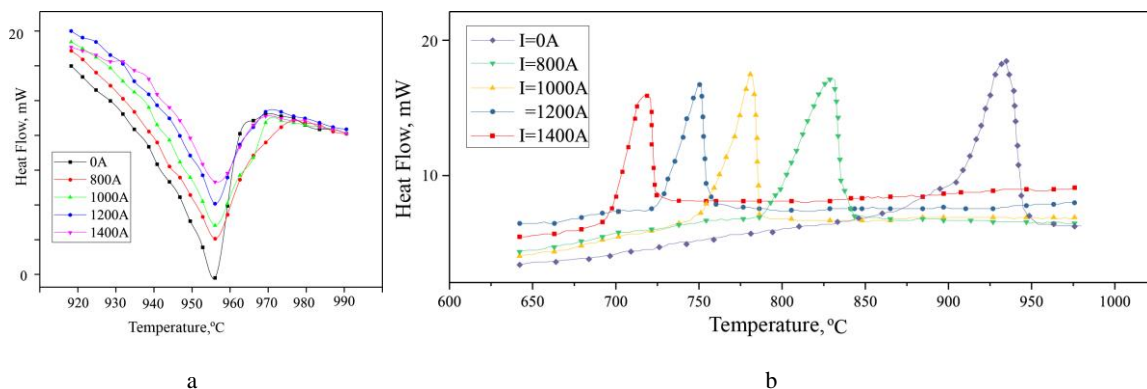


Fig. 6. DSC curves of Cu-37.4wt.%Pb alloy with various pulse current peaks: a – heating curve e; b – cooling curve

Table 3. Differential thermal analysis of Cu-37.4 wt.%Pb alloy treated with different pulsed currents

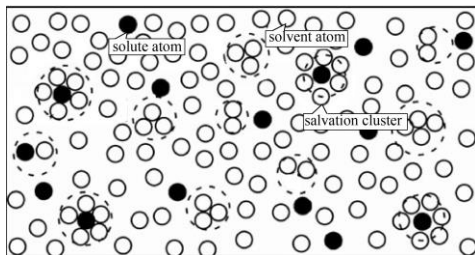
	I = 0 A	I = 800 A	I = 1000 A	I = 1200 A	I = 1400 A
Undercooling, K	24.6	120.1	137.7	163.2	179.6
Latent heat of fusion, J/g	202.1	170.8	163.9	149.3	138.5
Latent heat of the crystal, J/g	210.8	180.4	172.6	155.3	147.2
Melting temperature, °C	956.3	956.1	956.3	955.8	955.7
Solidification temperature, °C	930.4	834.9	817.3	791.8	775.4

Moreover, the number of large-scale “crystal embryos” that would meet the critical nucleus radius scale would increase, along with the amount of nucleation cores. This would further optimize the solidification structure of the metal [12, 17]. In the Cu-37.4 wt.%Pb alloy melt, the Cu atoms, the Pb atoms, the Cu-Cu clusters, the Pb-Pb clusters and the Cu-Pb salvation clusters existed. In liquid alloys, the solvents and solutes have a positive ion effect and a negative ion effect, respectively, due to the difference in electronegativity. According to thermodynamic properties, the salvation clusters were more stable than the solute and solvent clusters [12]. Therefore, when ECP was applied, smaller-scale solvent clusters might form new lower-sized volumes of salvation clusters with solute atoms. As a transformation result, the number of Cu-Pb clusters increased, along with the average interaction force among solvent atoms and solute atoms. This resulted in an activity decrease of each component in the metal melt and consequently weakened the segregation during solidification. The activity of the metal melt reflected the ability of the components in the melt to participate in the reaction. Through the ECP treatment, the numbers of dissociated individual atoms in the Cu-Pb alloy melt decreased, while most atoms were stable in the form of Cu-Pb clusters. It was proved that the ECP improved the solid solubility of the Cu-Pb monotectic alloy. Fig. 7 presents a schematic diagram of the alloy melt structure change under the action of ECP.

According to the Miedema formation heat model [18], the equation for the activity is:

$$\ln \gamma_i = \frac{\alpha_{ij}}{RT} \left[\Delta H_{ij} + (1-x_i) \frac{\partial \Delta H_{ij}}{\partial x_i} \right], \quad (1)$$

where γ_i is the activity coefficient; ΔH_{ij} is the mixing enthalpy; x_i is the molar volume fraction. Eq. 1 presents that the activity coefficients of Cu and Pb in the metal melt were related to the mixing enthalpy. According to the metal thermodynamics, the free energy change from one phase to another at a certain temperature is given by [19]:



a

$$\Delta G = \Delta H - T \Delta S, \quad (2)$$

If ΔG_V for the liquid to solid phase transformation of the free energy change per unit volume, then

$$G_V = G_S - G_L, \quad (3)$$

where G_S and G_L are the unit volume free energy of the solid phase and the unit volume free energy of the liquid phase, respectively, since:

$$G = H - TS, \quad (4)$$

The ΔG_V could be expressed as:

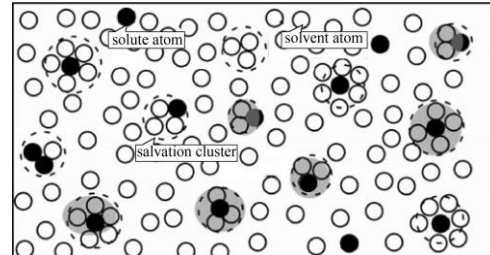
$$\Delta G_V = (H_S - H_L) - T(S_S - S_L). \quad (5)$$

The relationship under the constant pressure conditions is:

$$\Delta H_P = H_S - H_L = -L_m, \quad (6)$$

where L_m is the latent heat of fusion, ΔH is the mixing enthalpy of the melt. Based on the DSC curve presented in Fig. 6 and the calculated result in Table 2, the latent heat of fusion of the sample without ECP treatment was significantly lower compared to the samples with ECP treatments. Also, the latent heat of fusion decreased as the peak value increased. Therefore, under the action of the ECP, the mixing enthalpy of the metal melt decreased, while the activity coefficients of Cu and Pb in the metal melt decreased. This signified that the activity of both Cu and Pb decreased. The DSC curve confirmed the consistency and rationality of the latter analysis, proving that the ECP treatment increased the solid solubility of metal melt from the thermodynamic point of view.

In metal thermodynamics, the solid-state melting entropy ΔS_m is the melting entropy and it is expressed as [20]:



b

Fig. 7. Alloy melt structure transformation under ECP treatment s: a–before ECP treatment; b – after ECP treatment

Table 4. Hardness, friction coefficient and wear rate of Cu-37.4 wt. %Pb alloy treated with different pulsed currents

	I = 0 A	I = 800 A	I = 1000 A	I = 1200 A	I = 1400 A
Hardness, kgf·mm ⁻²	34.3	40.5	42.7	43.4	49.3
Friction coefficient	0.24	0.23	0.21	0.20	0.18
Wear rate	1.3	1.0	0.9	0.7	0.4

$$\Delta S_m = S_S - S_L = -L_m/T \quad (7)$$

This equation reflects the configuration entropy increase when the solid state changes to the liquid phase, while the value is the ratio of latent heat of melting to the melting point. Entropy is actually a measure of disorder. The high entropy represents a high degree of disorder in the melt. According to Fig. 6 and Table 2, it could be concluded that the latent heat of fusion of the sample without ECP treatment was lower compared to the samples with ECP treatment ($L'_m < L_m$). Combined with Eq. 7, it could be observed that $\Delta S'_m$ (with ECP) $<$ ΔS_m (without ECP). The melting entropy decrease of the modified samples indicated that the Cu-37.4 wt.%Pb alloy melt disorder degree decreased and the order degree increased. This was consistent with the conclusion that the action of ECP reduced the metal melt activity. It was also proved that with ECP treatment, the solid solubility of the Cu-37.4 wt.% Pb monotectic alloy melt was improved. Also, as the peak current increased, the solid solution effect was more apparent.

Viscosity is an important physical quantity, representing the interatomic force and momentum transfer in the liquid metal, also reflecting the binding force and interaction force among atomic groups in the metal melt. Based on the Yokoyama model [20], the following relationships among entropy S , diffusion coefficient D and viscosity η exist:

$$D = 0.049\sigma^2 \exp S; \quad (8)$$

$$\eta = k_B T / (2\pi\sigma D) \quad (9)$$

Subsequently to the ECP treatment, the Cu-37.4 wt.%Pb alloy entropy decreased, while in combination with Eq. 8 and Eq. 9, it could be inferred that the gold melt viscosity increased. This verified the ECP mechanism to improve the solid solubility of the metal, from the perspective of physical property change of the melt.

Table 4 shows the hardness, friction coefficient and wear rates of Cu-37.4 wt.%Pb monotectic alloys which treated with different current peaks. The results show that under the action of pulse current, the hardness of alloy increases, the friction coefficient and the wear rate decreases. As the peak value increases, the properties of anti-friction and wear-resistance of Cu-37.4 wt.%Pb alloys were enhanced.

4. CONCLUSIONS

The ECP demonstrated a high effect on the microstructure formation of a Cu-37.4 wt.% Pb alloy. The ECP treatment could significantly improve the

solidification structure of the Cu-Pb monotectic alloy, such as with fine microstructure, even distribution of the Pb phase in the Cu matrix, along with apparent solute trapping. The solid solubility of Pb in the Cu matrix increased. As the ECP peak value gradually increased, the solute trapping effect became more discrete.

According to the metal liquid cluster theory under pulsed electric field, the grain refinement could be a result of the presence of the increasing number of large-scale “embryos” that reached a critical radius; also, the solid solubility increase occurred due to the increase in salvation clusters under the action of pulse current. This led to the binding force increase among solute and solvent atoms.

Through the DSC curve analysis, the decrease in the cluster activity in the alloy melt was verified. The result revealed the mutual action between electric pulse modification and alloy melt structure to a certain extent.

The results of hardness test, anti-friction test and wear-resistance test analysis show that the ECP can improve the hardness of Cu-37.4 wt.%Pb alloy, the properties of anti-friction and wear-resistance of the alloy. As the peak value of the pulse current increases, the above properties of the Cu-37.4 wt.%Pb alloy are enhanced.

Acknowledgments

This work was supported by National Natural Science Foundation of China (grant number 51561001 and 51574171) and the Natural Science Foundation of Shanxi Province of China (grant number.201601D011012 and 2015011002).

REFERENCES

1. **Munitz, A., Landau, P., Kaufman, M., Abbaschian, R.** Microstructure and Phase Selection in Supercooled Copper Alloys Exhibiting Metastable Liquid Miscibility Gaps *Journal of Materials Science* 47 2012: pp. 7955–7970. <https://dx.doi.org/10.1007/s10853-012-6354-x>
2. **Molian, P.A., Buchanan, V.E., Sudarshan, T.S., Akers, A.** Sliding Wear Characteristics of Non-equilibrium Cu-Pb Alloys *Wear* 146 1991: pp. 257–267. [https://doi.org/10.1016/0043-1648\(91\)90067-5](https://doi.org/10.1016/0043-1648(91)90067-5)
3. **Buchanan, V.E., Molian, P.A., Sudarshan, T.S., Akers, A.** Frictional Behavior of Non-equilibrium Cu-Pb alloys *Wear* 146 1991: pp. 241–256. [https://doi.org/10.1016/0043-1648\(91\)90066-4](https://doi.org/10.1016/0043-1648(91)90066-4)
4. **Samuel, A.M., Garza-Elizondo, G.H., Doty, H.W., Samuel, F.H.** Role of Modification and Melt Thermal Treatment Processes on the Microstructure and Tensile Properties of Al-Si Alloys *Materials & Design* 80 2015: pp. 99–108. <https://doi.org/10.1016/j.matdes.2015.05.013>
5. **Tebib, M., Samuel, A.M., Ajersch, F., Chen, X.G.** Effect of P and Sr Additions on the Microstructure of

- Hypereutectic Al-15Si-14Mg-4Cu Alloy *Materials Characterization* 89 (3) 2014: pp. 112–123.
<https://doi.org/10.1016/j.matchar.2014.01.005>
6. **Liao, X., Zhai, Q., Luo, J., Chen, W., Gong, Y.** Refining Mechanism of the Electric Current Pulse on the Solidification Structure of Pure Aluminum. *Acta Materialia* 55 (9) 2007: pp. 3103–3109.
<https://doi.org/10.1016/j.actamat.2007.01.014>
 7. **Räbiger, D., Zhang, Y., Galindo, V., Willers, B., Eckert, S.** The Relevance of Melt Convection to Grain Refinement in Al-Si Alloys Solidified under the Impact of Electric Currents *Acta Materialia* 79 (41) 2014: pp. 327–338.
<https://doi.org/10.1016/j.actamat.2014.07.037>
 8. **Zhang, Y., Cheng, X., Zhong, H.** Comparative Study on the Grain Refinement of Al-Si Alloy Solidified under the Impact of Pulsed Electric Current and Travelling Magnetic Field *Metals* 6 2016: pp. 170.
<https://doi.org/10.3390/met6070170>
 9. **Jiang, H., Zhao, J., Wang, C., X, Liu.** Effect of Electric Current Pulses on Solidification of Immiscible Alloys *Materials Letters* 132 2014: pp. 66–69.
<https://doi.org/10.1016/j.matlet.2014.06.017>
 10. **Ma, J., Li, J., Gao, Y., Jia, L., Li, Z., Zhai, Q.** Effect of Peak Value and Discharge Frequency of Electric Current Pulse on Solidification Structure of Fe-1C-1.5Cr Bearing Steel *Ironmaking & Steelmaking* 36 (4) 2013: pp. 286–290.
<https://doi.org/10.1179/174328108x380654>
 11. **Zhao, Z., Su, J., Liu, Y.** The Electromagnetic Mechanism of Pulsed Electric Discharge on Directionally Solidified Microstructure of Pure Aluminum *Advanced Materials Research* 146–147 2011: pp. 297–300.
<https://doi.org/10.4028/www.scientific.net/amr.146-147.297>
 12. **Wang, J., Qi, J., Zhao, Z., Guo, H., Zhao, T.** Effects of Electric Pulse Modification on Liquid Structure of Al-5%Cu Alloy *Transactions of Nonferrous Metals Society of China* 23 2013: pp. 2792–2796.
[https://doi.org/10.1016/s1003-6326\(13\)62799-5](https://doi.org/10.1016/s1003-6326(13)62799-5)
 13. **Qi, J., Wang, J., He, L., Zhao, Z., Du, H.** An Investigation for Structure Transformation in Electric Pulse Modified Liquid Aluminum *Physical B Condensed Matter* 406 2011: pp. 846–849.
<https://doi.org/10.1016/j.physb.2010.12.010>
 14. **Zhao, Z., Wang, J., Liu, L.** Grain Refinement by Pulse Electric Discharging and Undercooling Mechanism *Materials and Manufacturing Processes* 26 (1) 2011: pp. 249–254.
<https://doi.org/10.1080/10426914.2010.512649>
 15. **Stepanov, G.V., Babutskii, A.I., Mameev, I.A.** High-Density Pulse Current-Induced Unsteady Stress-Strain State in a Long Rod *Strength of Materials* 36 (4) 2004: pp. 377–381.
<https://doi.org/10.1023/b:stom.0000041538.10830.34>
 16. **Cao, F., Xia, F., Hou, H., Ding, H., Li, Z.** Effects of High-Density Pulse Current on Mechanical Properties and Microstructure in a Rolled Mg–9.3Li–1.79Al–1.61Zn Alloy *Materials Science & Engineering A* 637 2015: pp. 89–97.
<https://doi.org/10.1016/j.msea.2015.03.127>
 17. **Wang, J.** Research of Treating Technology with Electropulse Modification and the Hypothesis of Liquid Metal Cluster Structure *Ph.D. dissertation University of Science and Technology* 1998 Beijing.
 18. **Miedema, A.R.** The Electronegativity Parameter for Transition Metals: Heat of Formation and Charge Transfer in Alloys *Journal of The Less-Common Met* 32 1973: pp. 117–136.
[https://doi.org/10.1016/0022-5088\(73\)90078-7](https://doi.org/10.1016/0022-5088(73)90078-7)
 19. **Wang, J.** Effect of ECP Treatment on Solidification Structure and Properties of Nonferrous Metals *Beijing (BY): Science Press* 2011.
 20. **Yoloyama, I.** Correlation Entropy and its Relation to Properties of Simple Liquid Metals *Journal of Non-Crystalline Solids* 312 (1) 2002: pp. 232–235.
[https://doi.org/10.1016/s0022-3093\(02\)01669-1](https://doi.org/10.1016/s0022-3093(02)01669-1)